ARC International, LLC

STABILITY OF BRACKET PLATES

Report for

IDEA StatiCa s.r.o.

August 26, 2022

Submitted by

Bo Dowswell, PE, PhD.
Principal
ARC International, LLC
(205) 283-2078
bo@arcstructural.com

Clayton Cox
Auburn University
Auburn Alabama

TABLE OF CONTENTS

INTRODUCTION

Brackets are used to transfer loads in steel structures where the load is offset from the support. Although rolled shapes can be used, brackets are usually fabricated from plates. Welded brackets are composed of a seat plate and a stiffener plate forming a T-shape as shown in Figure 1. The seat plate is welded to the stiffener plate and the stiffener plate is connected to the supporting member, typically by welding. Where practical, the seat plate is also connected to the support.

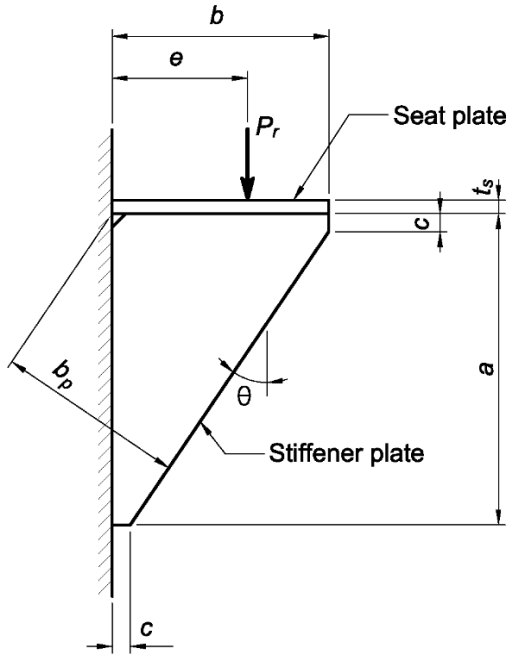

Fig. 1. Typical welded bracket.

Although stiffener plates can be rectangular, the free edges are usually shaped by making a diagonal cut as shown in Figure 1. To provide an adequate shelf at the weld ends, stiffener plates are usually fabricated with small (typically about 1-in.) perpendicular cuts, *c*. If stability of the stiffener plate is an issue, the edge can be stiffened by welding a plate along the free edge. In some cases where a rectangular stiffener plate is used, the bracket cross section can form an I-shape, with a seat plate at the top of the stiffener plate and an additional horizontal plate at the bottom. This report will focus on T-shaped brackets.

Typical Bracket Connections

Brackets are often used as beam-to-column connections, where the beam is offset from the column centerline. The classic example is for crane buildings, where the crane girder must be offset from the column to allow proper crane travel. However, similar connections are also used as seated beam, truss and joist connections. Other bracket connections include stiffened moment connections (Lee, 2002; Murray and Sumner, 2003) and fin plate connections for beams transferring large axial loads (Dowswell, 2010) as shown in Figures 2 and 3, respectively. Base plates can also be stiffened, either to increase the compression strength as shown in Figure 4 (Blodgett, 1966) or to provide an anchor bolt chair to resist tension forces.

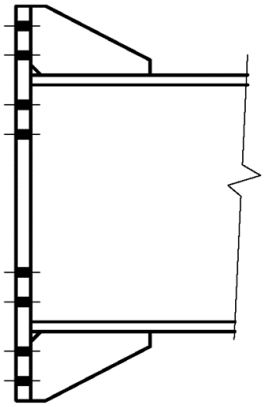

Fig. 2. End plate moment connection.

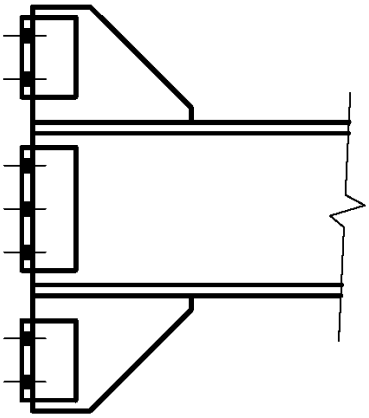

Fig. 3. Fin plate connection.

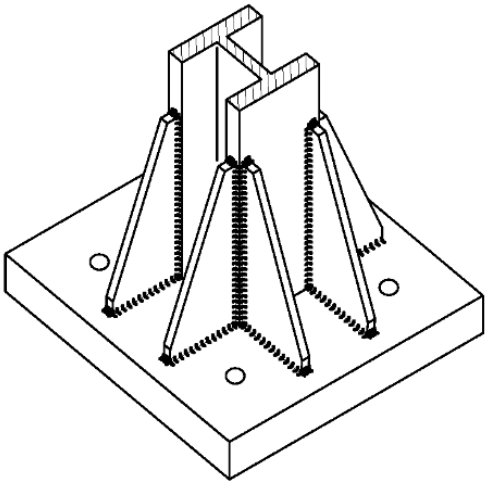

Fig. 4. Stiffened base plate.

Critical Section

The stiffener plate strength has traditionally been calculated at the critical section, which is the minimum width along the diagonal according to Equation 1.

$$b_p = \frac{ab - c^2}{\sqrt{(a-c)^2 + (b-c)^2}} \tag{1}$$

If the shelf cuts are neglected, the minimum width is

$$b_p = \frac{ab}{\sqrt{a^2 + b^2}} \tag{2}$$

where

a = stiffener plate depth, in.
b = stiffener plate width, in.
c = perpendicular shelf dimension, in.

Local Buckling

When designing elements that are subjected to compression stresses according to the AISC *Specification* (AISC, 2016a), engineers often limit the element slenderness to preclude local buckling. The limiting width-to-thickness ratios in *Specification* Tables B4.1a and B4.1b are based on the element geometry, loading and strain requirements. For element slenderness values greater than λ_r, the element is slender and local buckling must be considered in the design.

Calculation Design Method

The traditional design method uses mathematical equations to calculate the strength of structural elements and systems. Although accurate equations have been developed for most common conditions, only empirical or semi-empirical equations are available for some connection elements. For many conditions that are encountered in design practice, design guidance is unavailable. In these cases, simplified models are typically used to characterize the behavior of connection elements. Typically, these models are based on equations that were developed for beams, columns and tension members, where the assumptions used to derive the equations may not be satisfied in practice. Complex connections are often separated into Design Zones, which are isolated portions of the connection that are assumed to behave independently. Connection design models, which are based on the judgment of the engineer, can be inaccurate and can potentially lead to improper characterization of the behavior. For further information on this topic, see Dowswell (2020).

Finite Element Design Method

With proper modeling techniques, connections can be designed with finite element models. In most cases, connection resistance is defined by strength rather than deformation limits. Because connections typically have large stress concentrations, a material nonlinear analysis (MNA) is required for accurate prediction of the strength. For elements that are subjected to compression stresses, buckling can reduce the strength below that predicted by MNA. A linear buckling analysis (LBA) can provide information on the ideal elastic buckling behavior of connections. However, an accurate buckling analysis would include second-order effects (geometric nonlinearities), inelastic material behavior (material nonlinearities), geometric imperfections and residual stresses. Including these effects explicitly within

the analysis model requires a geometrically and materially nonlinear analysis with imperfections (GMNIA), which can significantly complicate the connection design process.

Accurate results can be obtained while achieving design efficiency by combining MNA with LBA. With this method, LBA results are used to determine the connection geometry that is required to eliminate buckling of the connection elements. Using this connection geometry, the strength is determined with MNA.

PROBLEM STATEMENT

A threshold critical load ratio has not been established for designing bracket plates to meet the AISC *Specification* requirements with LBA/MNA.

OBJECTIVE

The objective of this research is to develop practical design guidelines for the buckling strength of bracket plates that can be implemented with LBA/MNA.

PROCEDURE

The objective of this research was met by completing the following tasks:

1. Compile the experimental data from previous research projects
2. Determine the buckling force for each experimental specimen with LBA
3. Determine the inelastic strength of each experimental specimen with MNA
4. Calculate the strength of each experimental specimen with other design methods, including the 15th Edition AISC *Manual* design method
5. Determine an appropriate threshold critical load ratio for buckling of bracket plates
6. Using a first-order reliability analysis, calculate the reliability index for the LBA/MNA design method with the proposed critical load ratio

CALCULATION DESIGN METHOD

Common bracket design methods are summarized in this section of the report.

15th Edition AISC *Manual*

The design method in both the 14th Edition AISC *Steel Construction Manual* (AISC, 2011) and the 15th Edition AISC *Steel Construction Manual* (AISC, 2017) was derived using a simple mechanics approach. The stiffener plate is analyzed for flexural, axial and shear loads along the critical section, which is Section B-B in Figure 5.

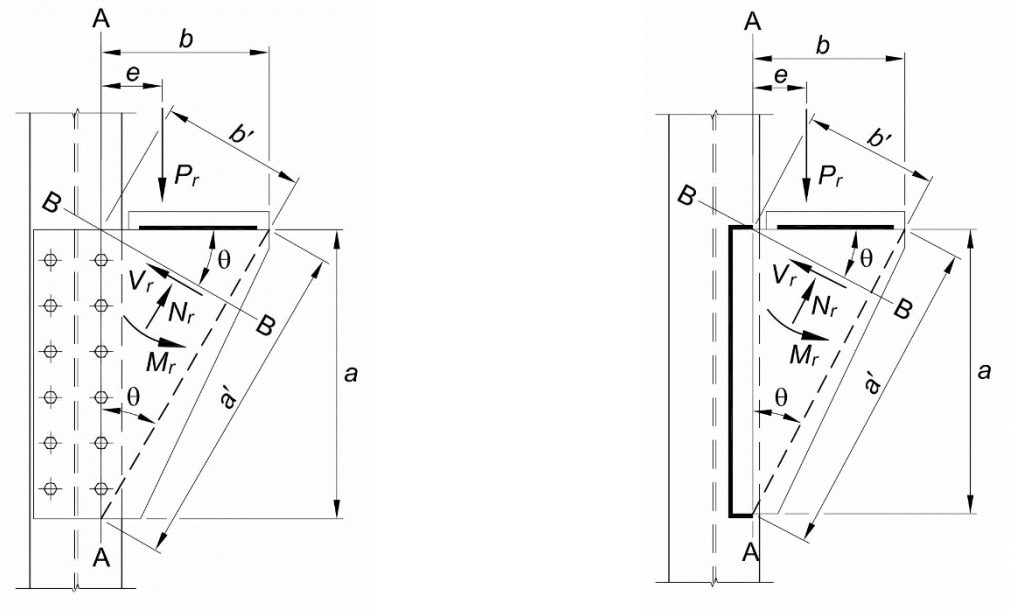

Fig. 5. Bracket plate connections in the 15th Ed. AISC Manual *(AISC, 2017).*

A similar connection is the stiffened seated connection shown in Figure 6. One of the differences between stiffened seated connections and bracket plates is the connection of the seat plate to the column. For stiffened seated connections, the seat plate is connected to the column to transfer a portion of the horizontal tension stress caused by the moment at the plate-to-column interface. For bracket plate connections, connecting the seat plate to the column is not required. The flexural strength increases significantly when the seat plate is connected to the column because the critical cross section is T-shaped rather than rectangular.

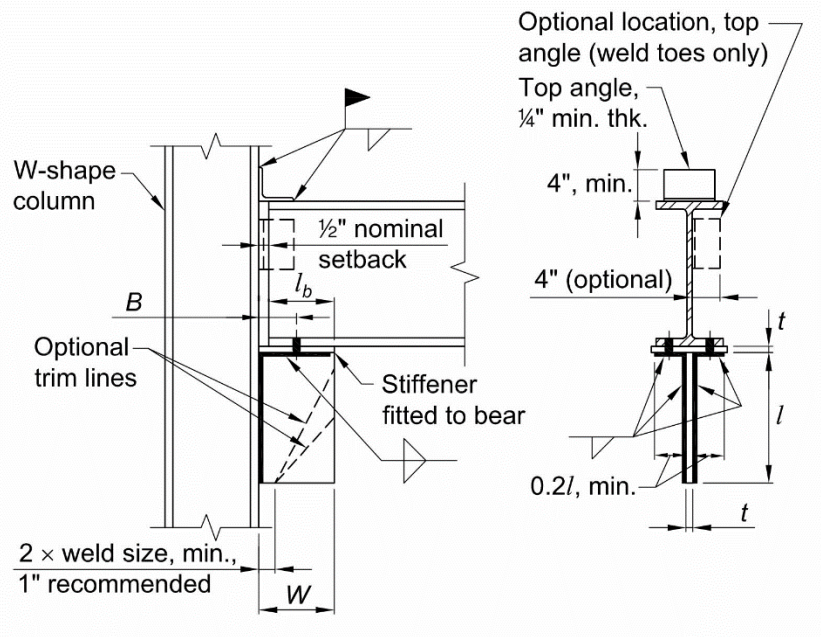

Fig. 6. Stiffened seated connection in the 15th Ed. AISC Manual *(AISC, 2017).*

The design method for stiffened seated connections has been used for many decades and has been verified by experimental tests. For seated connections that meet the requirements of *Manual* Part 10, the critical section is assumed to be along a horizontal plane in the bracket plate along the seat-to-bracket interface. Therefore, an evaluation of the section along the minimum diagonal width is not required.

For bracket connections, the combined axial and flexural loads along Section B-B are evaluated with linear interaction according to Equation 3.

$$\frac{N_r}{N_c} + \frac{M_r}{M_c} \leq 1.0 \tag{3}$$

The required axial and flexural loads are calculated with Equations 4 and 5, respectively.

$$N_r = P_r \cos \theta \tag{4}$$

$$M_r = P_r e - N_r \left(\frac{b'}{2} \right) \tag{5}$$

The nominal axial and flexural loads are calculated with Equations 6 and 7, respectively.

$$N_n = F_{cr} t b' \tag{6}$$

$$M_n = \frac{F_{cr} t b'^2}{4} \tag{7}$$

The critical stress is calculated with Equation 8.

$$F_{cr} = Q F_y \tag{8}$$

The effect of local buckling is considered with the reduction factor, Q, which varies with the slenderness parameter, λ. When $\lambda \leq 0.70$, the limit state of local buckling need not be considered and $Q = 1.00$. When $0.70 < \lambda \leq 1.41$

$$Q = 1.34 - 0.486\lambda \tag{9}$$

When $1.41 < \lambda$

$$Q = \frac{1.30}{\lambda^2} \tag{10}$$

The slenderness parameter is calculated with Equation 11.

$$\lambda = \frac{\left(\frac{b'}{t}\right)\sqrt{F_y}}{5\sqrt{475+1{,}120\left(\frac{b'}{a'}\right)^2}} \tag{11}$$

where

F_y = specified minimum yield stress, ksi
a' = stiffener plate free edge length, in.
b' = width of stiffener plate at the critical section, in.
t = stiffener plate thickness, in.
θ = angle of free edge from the vertical plane, degrees

The reduction and safety factors are $\phi = 0.90$ for LRFD design and $\Omega = 1.67$ for ASD design.

13th Edition AISC *Manual*

The design method in the 13th Edition *Manual* (AISC, 2005) was based on a theoretical investigation by Salmon (1962) and experimental tests by Salmon et al. (1964). The design method was modified and summarized by Salmon and Johnson (1990). The nominal yield load of the bracket is

$$P_n = F_y z b t \tag{12}$$

Where z is the ratio of the average stress on the loaded edge to the maximum stress on the free edge of the bracket plate. Equation 13, which was developed empirically by Salmon et al. (1964), can be used to calculate z.

$$z = 1.39 - 2.2\left(\frac{b}{a}\right) + 1.27\left(\frac{b}{a}\right)^2 - 0.25\left(\frac{b}{a}\right)^3 \tag{13}$$

Equation 12 is valid only if buckling of the bracket plate is prevented. The slenderness limits, which were originally suggested by Salmon and Johnson (1990), are

When $0.50 \le \frac{b}{a} \le 1.0$

$$\frac{b}{t} \le 1.47\sqrt{\frac{E}{F_y}} \tag{14}$$

When $1.0 < \frac{b}{a} \le 2.0$

$$\frac{b}{t} \le 1.47\sqrt{\frac{E}{F_y}}\left(\frac{b}{a}\right) \tag{15}$$

where

E = modulus of elasticity, ksi

The assumptions made in the development of these equations are:
1. The seat plate is rigidly attached to the support
2. The load is distributed along the seat plate with a centroid at 0.6*b* from the support
3. $0.50 \le b/a \le 2.0$

Tall et al. (1964)
The mechanics approach used in the 15th Edition AISC *Steel Construction Manual* (AISC, 2017) was originally developed by Tall et al. (1964), who derived equations for both elastic and plastic strengths at the critical section. The elastic method was also discussed by Blodgett (1966). Stability of the stiffener plate was ensured by limiting the slenderness, *b*/*t*. The plastic method is applicable when

$$\frac{b}{t} \le \frac{48 + 24\left(b/a\right)}{\sqrt{F_y}} \tag{16}$$

For larger *b*/*t* ratios, the elastic method is applicable; however, the following slenderness limits must be met

When $0.50 \le \frac{b}{a} \le 1.0$

$$\frac{b}{t} \le \frac{180}{\sqrt{F_y}} \tag{17}$$

When $1.0 < \frac{b}{a} \le 2.0$

$$\frac{b}{t} \le \frac{60 + 120\left(b/a\right)}{\sqrt{F_y}} \tag{18}$$

Other Design Methods
Shakya and Vinnakota (2008) developed design tables that were based on summing the flexural buckling strength of unit-width column strips oriented parallel to the bracket plate free edge. Several of the publications discussed in the following sections of this report proposed similar design methods. Laustsen et al. (2012) developed a method to calculate the compression strength of triangular bracket plates using the yield line method.

LOCAL BUCKLING OF CONNECTION ELEMENTS

This section of the report provides information on the local buckling of connection elements.

Slenderness Limits
Limiting width-to-thickness ratios are listed for various compression elements in AISC *Specification* Tables B4.1a and B4.1b. Although the development of these values relied heavily on experimental

testing (AISC, 2020), the noncompact slenderness limit, λ_r, can be determined using the critical buckling stress according to Equation 19 (Bryan, 1891).

$$\sigma_c = \frac{\pi^2 Ek}{12\left(1-\nu^2\right)}\left(\frac{t}{b}\right)^2 \tag{19}$$

where

b = element width, in.
k = buckling coefficient
t = element thickness, in.
ν = Poisson's ratio

The noncompact limit can be determined by solving Equation 19 for b/t, substituting F_y for σ_c, and multiplying by a reduction factor, α_r, to account for residual stresses and geometric imperfections. The resulting noncompact limit is

$$\lambda_r = \pi\alpha_r\sqrt{\frac{kE}{12\left(1-\nu^2\right)F_y}} \tag{20}$$

Substituting $\alpha_r = 0.7$, which was used to develop the AISC *Specification* nonslender limits, into Equation 20 results in Equation 21.

$$\lambda_r = 0.665\sqrt{\frac{kE}{F_y}} \tag{21}$$

For rectangular connection elements, the slenderness is defined as $\lambda = b/t$. However, the slenderness of triangular elements can be defined using either the perpendicular width, b, or the width at the critical section, b_p, as shown in Figure 1. As discussed previously, the critical section width is used for bracket plate connections in the 15th Ed. AISC *Manual* (AISC, 2017). For end plate moment connections (Figure 2), both AISC Design Guide 4 (Murray and Sumner, 2003) and AISC 358-16 (AISC, 2016b) limit the stiffener slenderness based on the perpendicular width per Equation 22.

$$\frac{h_{st}}{t_s} \le 0.56\sqrt{\frac{E}{F_{ys}}} \tag{22}$$

where

F_{ys} = specified minimum yield stress of the stiffener, ksi
h_{st} = stiffener height, in.
t_s = stiffener thickness, in.

Buckling Coefficients

Buckling coefficients are dependent on the element shape, the load distribution and the boundary conditions. For infinitely-long rectangular elements loaded uniformly at two edges as shown in Figure 7, the buckling coefficients are (Ziemian, 2010):

k = 0.425 when the non-loaded edges are pinned-free
k = 1.33 when the non-loaded edges are fixed-free

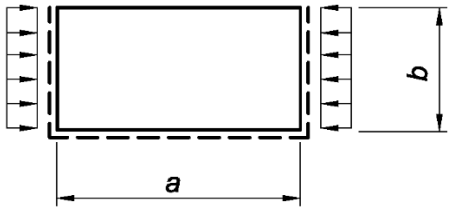

Fig. 7. Plate buckling model.

Generally, it was determined that the slenderness limits in AISC *Specification* Tables B4.1a and B4.1b can be estimated with buckling coefficients that are between the pinned and fixed values (AISC, 2020). Gerard and Becker (1957) derived equations for finite-length rectangular plates loaded uniformly at two edges with a non-loaded edge free (Figure 7).

For plates with three edges pinned

$$k = 0.425 + \left(\frac{b}{a}\right)^2 \tag{23}$$

Equation 11 was developed by Muir and Thornton (2004) based on Equation 23. For plates with three edges fixed

$$k = 0.551 + 0.136\left(\frac{a}{mb}\right)^2 + 0.987\left(\frac{mb}{a}\right)^2 \tag{24}$$

where
a = plate length, in.
m = integer that results in the lowest plate buckling coefficient (m = 1 for a/b < 2.32)

ABS (2004) suggested that the buckling strength of triangular bracket plates can be estimated with equations that were developed for rectangular plates by substituting b = 2/3 times the width of the critical section (b_p in Figure 1) and a = 2/3 times the free edge length (a' in Figure 5).

Salmon et al. (1964) recommended Equation 25 for the design of triangular stiffener plates in bracket connections. The empirical equation results in a lower-bound to experimental tests and a theoretical elastic buckling analysis by Salmon (1962), which included both fixed and pinned boundary conditions at the two supported plate edges. The theoretical and experimental research used a distributed load along the seat plate with a centroid at 0.6b from the support. The equation has a range of validity of $0.75 \le b/a \le 2.0$ and was calibrated for use with the average stress on the loaded edge, $\sigma = P_r/(bt)$.

$$k = 3.2 - 3.0\left(\frac{b}{a}\right) + 1.1\left(\frac{b}{a}\right)^2 \tag{25}$$

Table 4.2 of EN 1993-1-5: 2006 (CEN, 2006) has equations for the buckling coefficients of unstiffened elements with linearly varying stresses across the element width.

Buckling Stress

AISC *Specification* Section E7 addresses the strength of compression members with slender elements.

When $\lambda \le \lambda_r \sqrt{\frac{F_y}{F_{cr}}}$

$$b_e = b \tag{26}$$

When $\lambda > \lambda_r \sqrt{\frac{F_y}{F_{cr}}}$

$$b_e = b\left(1 - c_1\sqrt{\frac{F_{el}}{F_{cr}}}\right)\sqrt{\frac{F_{el}}{F_{cr}}} \tag{27}$$

where

F_{cr} = critical stress for global member buckling, ksi
F_{el} = elastic local buckling stress, ksi
b_e = element effective width, in.
c_1 = imperfection adjustment factor

From AISC *Specification* Table E7-1, $c_1 = 0.22$. For local buckling without global member buckling, $F_{cr} = F_y$. An equivalent stress reduction factor can be determined by substituting these values into Equation 27 and solving for b_e/b, resulting in Equation 28.

$$\begin{aligned}\rho &= \frac{b_e}{b} \\ &= \frac{\left(1 - 0.22/\alpha\right)}{\alpha}\end{aligned} \tag{28}$$

Where the slenderness parameter is

$$\alpha = \sqrt{\frac{F_y}{F_{el}}} \tag{29}$$

When $\alpha > 0.673$, ρ is calculated with Equation 28. When $\alpha \le 0.673$, $\rho = 1.00$. The boundary value of $\alpha = 0.673$ between first yield and local buckling behavior was first developed by Winter (1947). The buckling reduction factor is plotted in Figure 8.

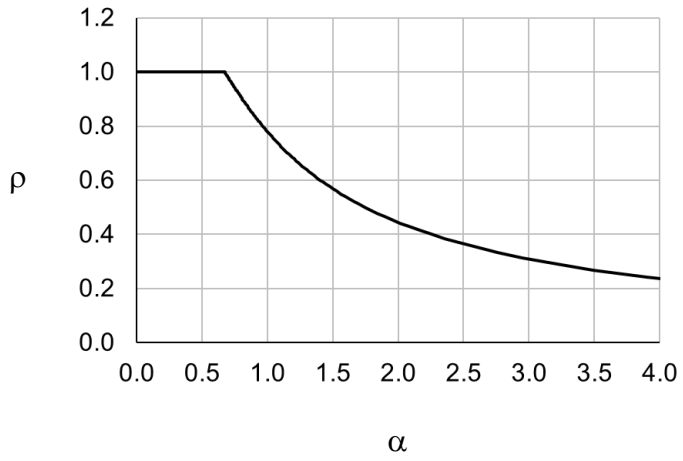

Fig. 8. Buckling reduction factor versus element slenderness.

For design assisted by finite element analysis, Section 8.1.4.1 of EN 1993-1-14 (CEN, 2020) defines the slenderness parameter as

$$\alpha = \sqrt{\frac{R_p}{R_e}} \tag{30}$$

where

R_e = critical buckling resistance determined with a linear elastic bifurcation analysis (LBA)

R_p = plastic resistance determined with a material nonlinear analysis (MNA). A conservative estimate can be obtained using a linear elastic analysis (LA)

Kurikova et al. (2019) noted that the slenderness parameter can also be expressed using Equation 31.

$$\alpha = \sqrt{\frac{\alpha_p}{\alpha_e}} \tag{31}$$

where

α_e = critical buckling factor determined with a linear elastic bifurcation analysis (LBA)

α_p = plastic resistance factor determined with a material nonlinear analysis (MNA). A conservative estimate can be obtained using the first-yield resistance from a linear elastic analysis (LA), α_y.

Critical Stress Ratios

For elements in members subjected to axial compression, the limiting nonslender width-to-thickness ratios in *Specification* Table B4.1a correspond to $\alpha_r = 0.7$, which results in $F_{el}/F_y = 2.04$ (Seif and Schafer, 2010). This agrees well with the experimental results, which indicated that $F_{el}/F_y \approx 2$ is necessary to reach the first yield strength without buckling (AISC, 2020). For Equation 26 (as well as Equations 27 and 28), $\alpha_r = 0.673$, which results in $F_{el}/F_y = 2.21$.

For elements in members subjected to flexural compression, the limiting noncompact width-to-thickness ratios in *Specification* Table B4.1b correspond to either $\alpha_r = 0.7$ or $\alpha_r = 1.0$ (AISC, 2020). The limiting compact width-to-thickness ratios must allow adequate inelastic strain capacity for the entire cross section to reach the plastic flexural strength. The limiting noncompact width-to-thickness ratios in *Specification* Table B4.1b correspond to $\alpha_p = 0.464$ for unstiffened elements which results in $F_{el}/F_y = 4.64$ (AISC, 2020).

As part of the Continuous Strength Method (CSM), Fieber et al. (2019) developed a continuous curve to predict the strain capacity of compression elements as a function of the element slenderness parameter, α. The curve is defined by two parts, nonslender and slender, which are separated at $\alpha_r = 0.68$ and defined by Equations 32 and 33, respectively. Additionally, a maximum strain ratio, Ω, is specified for Equation 32. The authors recommended $\Omega = 15$ based on CEN (2005) Section 3.2.2; however, Section 3.2.2 also requires a rupture elongation of not less than 15%. Fieber et al. (2019) noted that $\Omega = 30$ may be appropriate where "extensive plasticity is tolerable at the ultimate limit state and a suitably ductile steel is being used." Because connections are designed at the strength level, generally without regard for deformations, it is anticipated that most connections can be designed with $\Omega = 30$. The equations were calibrated against tests on beams and stub columns; therefore, the effects of residual stresses and geometric imperfections are implicitly considered.

For $\alpha \leq 0.68$

$$\frac{\varepsilon_{csm}}{\varepsilon_y} = \frac{1}{4\alpha^{3.6}} \leq \Omega \tag{32}$$

For $\alpha > 0.68$

$$\frac{\varepsilon_{csm}}{\varepsilon_y} = \left(1 - \frac{0.222}{\alpha^{1.05}}\right)\frac{1}{\alpha^{1.05}} \tag{33}$$

Equation 32 can be solved for α, resulting in Equation 34.

$$\alpha_{csm} = \left[\frac{1}{4\left(\varepsilon_{csm}/\varepsilon_y\right)}\right]^{\frac{1}{3.6}} \tag{34}$$

Columns 2 and 3 of Table 1 list α_{csm} and F_{el}/F_y, respectively, for various strain ratios, $\varepsilon_{csm}/\varepsilon_y$. Additionally, the strain at $F_y = 50$ ksi, ε_{50}, is listed in Column 4.

Table 1. Slenderness parameters based on the Continuous Strength Method.				
$\varepsilon_{csm}/\varepsilon_y$	α_{csm}	F_{el}/F_y	ε_{50} (%)	Comments
0.90	0.7	2.0	0.156	AISC Table B4.1a nonslender limit
1	0.68	2.16	0.172	CSM nonslender limit
1.81	0.577	3	0.311	
3.03	0.500	4	0.523	
3.97	0.464	4.64	0.684	AISC Table B4.1b unstiffened noncompact limit
8.73	0.373	7.20	1.50	Initiation of strain hardening (FEMA, 2000)
15.0	0.321	9.72	2.59	CEN (2005) strain ratio limit
17.4	0.308	10.6	3	
23.2	0.284	12.4	4	
29.0	0.267	14.0	5	
30	0.265	14.3	5.17	Fieber et al. (2019)
$\varepsilon_{50} = \varepsilon_{csm}$ for F_y = 50 ksi (%)				

The limiting noncompact width-to-thickness ratios in *Specification* Table B4.1b are intended to provide adequate ductility for the element to reach the initial point of strain hardening (AISC, 2020). However, Equation 31 results in a strain ratio of 3.97, which is lower than the minimum experimental strain hardening ratio of 4.29 reported by FEMA (2000) and significantly lower than the mean value of 8.73. Because the CSM equations were developed for elements in axial compression, they may be inaccurate for elements, such as bracket plates, with significant strain gradients.

PREVIOUS BRACKET RESEARCH

This section of the report provides a review of the previous research projects on brackets. The research included theoretical analyses, finite element models and experimental tests. From the experimental research, sufficient data was available to include 86 of the specimens in this report. The specimen details and test results are listed in Appendix A Table A1.

Theoretical Analyses

Salmon (1962) developed theoretical solution to determine the buckling strength of triangular bracket plates using the Rayleigh-Ritz energy method. The stress distribution within the bracket was determined first, and then the elastic buckling load was based on the stresses. The bracket plate interfaces at the support and the seat plate were modeled with two restraint conditions: simply supported and fixed. A total of 61 different conditions were studied.

Experimental Tests

15 experimental specimens were tested by Salmon et al. (1964). The specimens used triangular bracket plates with b/a ratios between 0.75 and 2.0. The experimental results showed that the ultimate loads were from 70% to 400% higher than the first yield loads for the specimens that failed by inelastic buckling. Both the experiments and theoretical models used a load centroid located at a distance of $0.6b$ from the support. Equation 13 was developed empirically to closely approximate the experimental stresses at the free edge of the bracket plate, which were significantly higher than the theoretical stresses calculated by Salmon (1962). The equation predicts the ratio of the average stress at the loaded (horizontal) edge to the maximum stress at the free edge.

20 experimental specimens were tested by Jensen (1936); however, these tests were excluded from Table A1 because the reported data was insufficient.

Martin (1979) tested seven specimens and Robinson (1983) tested many different bracket plate connections, including some tests that failed by weld rupture. Several of these tests were also reported by Martin and Robinson (1981). All of the tests by Martin (1979) and 61 of the tests by Robinson (1981) were used in this study.

Kurejkova and Wald (2017) tested six specimens; however, three of the specimens were stiffened at the free edges. Therefore, only the three non-stiffened specimens were considered in this report.

Finite Element Models

Wu and Wang (1996) and Hsu (1986) used finite element models with a linear elastic bifurcation analysis (LBA) to study the behavior of brackets. The research by Kurejkova and Wald (2017) and Pasternak and Kocker (1995) used similar finite element models with nonlinear material models.

FINITE ELEMENT DESIGN METHOD

Accurate results can be achieved with the finite element method by combining MNA with LBA. Because a valid design strength can be determined from MNA only if buckling is eliminated, a limit on the LBA critical load must be satisfied. This limit can be in the form of a critical load ratio, P_{el}/P_r, where P_r is the required force and P_{el} is the elastic buckling force from LBA.

An appropriate finite element design method for bracket connections will be established by comparing the available experimental results to corresponding LBA/MNA models built with IDEA StatiCa software. A threshold critical load ratio will be established by comparing the maximum experimental forces, P_e, to those from LBA. Using the proposed critical load ratio, the accuracy of the design method will be verified with a first-order reliability analysis based on the results from MNA with a 5% strain limit.

RESULTS

Specimen details for 86 experimental tests from four previously published research projects are listed in Appendix A Table A1. Experimental and design results are listed in Table A2. At the maximum test load, the failure mode for all specimens was inelastic buckling of the free edge. Some of the specimens buckled in the elastic range but deformed plastically after further loading. The specimens typically behaved linearly over most of the loading range, followed by larger in-plane and out-of-plane inelastic deformations.

Calculation Design Method

Using the design method developed by Salmon et al. (1964) and the methods in both the 13th and 15th Edition AISC *Manuals*, the strength of each specimen was calculated and compared to the experimental results. The calculations were based on the measured material and geometric properties for each specimen.

For the Salmon et al. (1964) method, the bracket strength is calculated with Equations 12, 13, 19 and 25. Only 78 specimens met the limits of applicability for Equation 25, which has a range of validity of $0.75 \leq b/a \leq 2.0$. For these specimens, the mean experimental-to-calculated load ratio is 1.83 with a coefficient of variation of 0.409.

For the 15th Edition AISC *Manual* method, which has no limits of applicability, the bracket strength is calculated with Equations 3 through 11. Using all 86 specimens, the mean experimental-to-calculated load ratio is 3.20 with a coefficient of variation of 0.417.

For the 13th Edition AISC *Manual* method, the bracket strength is calculated with Equations 12, 13, 14 and 15. Only 25 specimens met both the b/t limits of Equations 14 and 15, and the range of applicability for Equation 13 ($0.50 \leq b/a \leq 2.0$). For these specimens, the mean experimental-to-calculated load ratio is 2.27 with a coefficient of variation of 0.348.

Finite Element Design Method

By comparing the maximum experimental forces to those from LBA, the proposed threshold critical load ratio, P_{el}/P_e, was determined. Figure 9 shows a plot of P_e/P_i versus P_{el}/P_e for all experimental specimens, where P_i is the inelastic strength based on 5% strain from MNA and P_{el} is the elastic buckling force from LBA. All models were built with the measured specimen geometries and material properties. The vertical red dashed line represents $P_{el}/P_e = 4$. For the 14 specimens with $P_{el}/P_e \geq 4$, two specimens have a P_e/P_i ratio less than 1.0. For $\phi = 0.90$, all 14 specimens are stronger than the LRFD available strength. Using the MNA results for the 14 specimens with $P_{el}/P_e \geq 4$, the average P_e/P_i ratio is 1.29 with a coefficient of variation of 0.224.

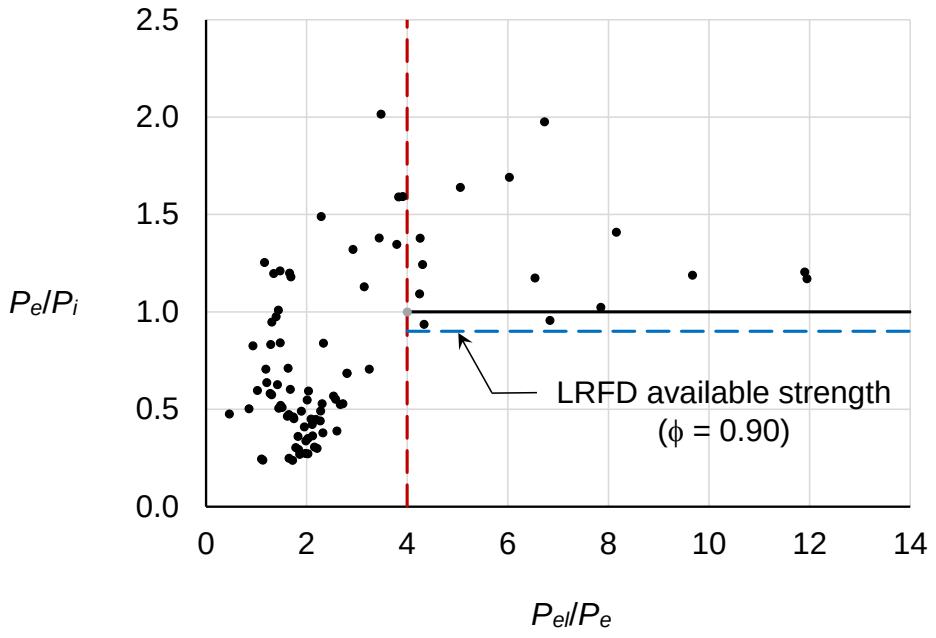

Fig. 9. Normalized experimental loads versus critical load ratio.

Figure 10 shows a plot of P_e/P_i versus α for all experimental specimens, with the buckling reduction factor from AISC *Specification* Section E7 plotted with solid black lines. The experimental trendline falls well below the *Specification* curve, indicating that the *Specification* curve will be non-conservative if applied to bracket plates.

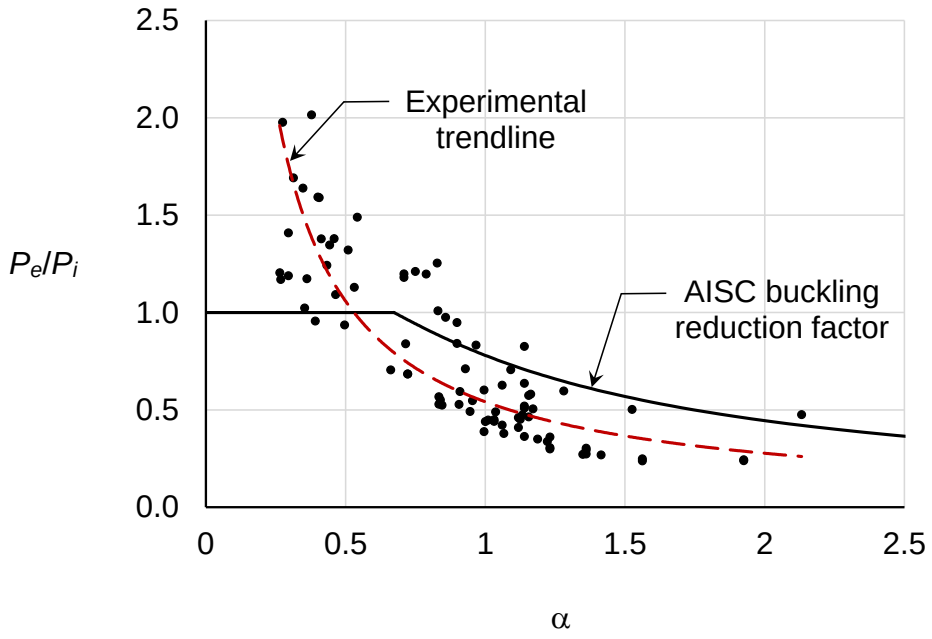

Fig. 10. Normalized experimental loads versus element slenderness.

Reliability Analysis

A reliability analysis was used to determine the required reduction factor, ϕ. The statistical parameters were based on the measured material and geometric properties of the experimental specimens. The reduction factor required to obtain a specific reliability level is (Galambos and Ravinda, 1978)

$$\phi = C_R \rho_R e^{-\beta \alpha_R V_R} \tag{35}$$

where

C_R = correction factor
V_R = coefficient of variation
α_R = separation factor
β = reliability index
ρ_R = bias coefficient

Galambos and Ravinda (1973) proposed a separation factor, α_R, of 0.55. For L/D = 3.0, Fisher et al. (1978) developed Equation 36 for calculating the correction factor.

$$C_R = 1.40 - 0.156\beta + 0.0078\beta^2 \tag{36}$$

The coefficient of variation and bias coefficient are calculated using the statistical parameters of the specific joint. The bias coefficient is

$$\rho_R = \rho_M \rho_G \rho_P \tag{37}$$

where

ρ_G = bias coefficient for the geometric properties
ρ_M = bias coefficient for the material properties

ρ_P = bias coefficient for the test-to-predicted strength ratios. Mean value of the professional factor calculated with the measured geometric and material properties.

The coefficient of variation is

$$V_R = \sqrt{V_M^2 + V_G^2 + V_P^2} \tag{38}$$

where

V_G = coefficient of variation for the geometric properties
V_M = coefficient of variation for the material properties
V_P = coefficient of variation for the test-to-predicted strength ratios

To consider the effect of small sample sizes, AISI (2016) uses a correction factor applied to V_p, resulting in a coefficient of variation of

$$V_R = \sqrt{V_M^2 + V_G^2 + C_p V_P^2} \tag{39}$$

The correction factor for $n \geq 4$ is

$$\begin{aligned} C_P &= \left(1 + \frac{1}{n}\right)\left(\frac{m}{m-2}\right) \\ &= \left(1 + \frac{1}{n}\right)\left(\frac{n-1}{n-3}\right) \end{aligned} \tag{40}$$

where

m = degrees of freedom
= $n - 1$
n = number of tests

Equation 40 was originally developed by Hall and Pekoz (1988) and revised by Tsai (1992). Hess et al. (2002) recommended $\rho_G = 1.05$ and $V_G = 0.044$ for plate thickness variations. For the plate yield strength, $\rho_M = 1.11$ and $V_M = 0.054$ (Schmidt and Bartlett, 2002). Using the MNA results for the 14 specimens with $P_{el}/P_e \geq 4$, $\rho_P = 1.29$ and $V_P = 0.224$. For $n = 14$, Equation 40 results in $C_p = 1.27$. For these parameters, $V_R = 0.261$ and $\rho_R = 1.51$. At $\phi = 0.90$, $\beta = 3.34$.

Based on the Commentary to *Specification* Section B3.1, the reliability indices for members and connections are 2.6 and 4.0, respectively. The ductile behavior and stable post-buckling response of bracket connections reduces the consequences of failure. Also, the suggested design method ensures ductile behavior by eliminating the buckling limit state. Therefore, a target reliability index, β_T, between 2.6 and 4.0 is appropriate for these conditions. The calculated $\beta = 3.34$ is approximately halfway between these two values.

SUMMARY AND CONCLUSIONS

The purpose of this research was to develop practical design guidelines for the buckling strength of bracket plates that can be implemented with LBA/MNA. Details of 86 experimental specimens from four previous research projects were compiled. For these 86 specimens, the design method in the 15th Edition AISC *Manual* was conservative, with a mean experimental-to-calculated load ratio of 3.20 and a coefficient of variation of 0.417. Finite element models corresponding to each experimental specimen were analyzed with both LBA and MNA to determine the buckling force and inelastic strength, respectively. A first-order reliability analysis revealed the accuracy of the design method and was used to verify an appropriate reduction factor for LRFD design. The results showed that accurate results can be achieved with the finite element method by combining MNA with LBA. To avoid buckling, the critical load, P_{el}, based on LBA, must be equal to or greater than $4P_r$ for LRFD design and $6P_r$ for ASD design. For the 14 specimens that satisfy this condition, a mean experimental-to-calculated load ratio is 1.27 and a coefficient of variation of 0.261. For these connections, the available strength is calculated using MNA at a 5% strain limit with $\phi = 0.90$ (LRFD) or $\Omega = 1.67$ (ASD).

DESIGN EXAMPLE

In this example, a W18×76 ASTM A992 beam is connected to a column flange with a bracket as shown in Figure 11. The bracket plate will be evaluated using both the 15th Edition AISC *Manual* design method and the finite element design method. The seat plate is w in. × 9 in. × 14 in. and the bracket plate is 2 in. × 14 in. × 18 in. All plates are ASTM A572 Gr. 50.

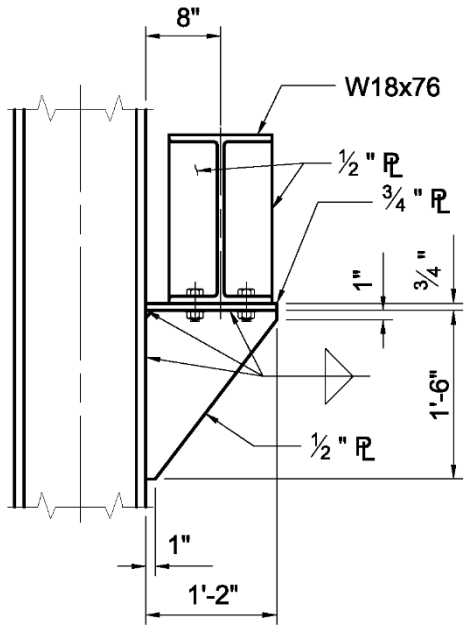

Fig. 11. Bracket connection for Design Example.

The required vertical shear reaction, P_r, is:

LRFD	ASD

P_u = 105 kips	P_a = 70 kips

Solution

A572 Gr. 50: F_y = 50 ksi

Seat plate dimensions: t_s = w in.

Bracket plate dimensions: t = 2 in. a = 18 in. b = 14 in. c = 1 in.

Eccentricity: e = 8 in.

Calculation Design Method

The design method in the 15th Edition AISC *Steel Construction Manual* (AISC, 2017) is based on the assumption that the seat plate is connected only to the bracket plate, any seat-plate-to-column weld is disregarded.

The angle from vertical is

$$\begin{aligned}\theta &= \tan^{-1}\left(\frac{b}{a}\right)\\ &= \tan^{-1}\left(\frac{14\,\text{in.}}{18\,\text{in.}}\right)\\ &= 37.9^\circ\end{aligned}$$

The length of the free edge is

$$\begin{aligned}a' &= \frac{a}{\cos\theta}\\ &= \frac{18\,\text{in.}}{\cos(37.9^\circ)}\\ &= 22.8\,\text{in.}\end{aligned}$$

The width of the critical section is

$$\begin{aligned}b' &= a\sin\theta\\ &= (18\,\text{in.})\sin(37.9^\circ)\\ &= 11.1\,\text{in.}\end{aligned}$$

The slenderness parameter is calculated with Equation 11.

$$\lambda = \frac{\left(\frac{b'}{t}\right)\sqrt{F_y}}{5\sqrt{475+1{,}120\left(\frac{b'}{a'}\right)^2}}$$

$$= \frac{\left(\frac{11.1\text{in.}}{0.500\text{in.}}\right)\sqrt{50\,\text{ksi}}}{5\sqrt{475+1{,}120\left(\frac{11.1\text{in.}}{22.8\text{in.}}\right)^2}}$$

$$= 1.15$$

The buckling reduction factor is calculated with Equation 9.

$$Q = 1.34 - 0.486\lambda$$
$$= 1.34 - 0.486(1.15)$$
$$= 0.781$$

The critical stress is calculated with Equation 8.

$$F_{cr} = QF_y$$
$$= (0.781)(50\text{ ksi})$$
$$= 39.1\text{ ksi}$$

The nominal axial force is calculated with Equation 6.

$$N_n = F_{cr}tb'$$
$$= (39.1\text{ ksi})(0.500\text{ in.})(11.1\text{ in.})$$
$$= 217\text{ kips}$$

The nominal flexural load is calculated with Equation 7.

$$M_n = \frac{F_{cr}tb'^2}{4}$$
$$= \frac{(39.1\text{ksi})(0.500\text{in.})(11.1\text{in.})^2}{4}$$
$$= 602\,\text{kip-in.}$$

The required axial force is calculated with Equation 4.

$$N_r = P_r \cos\theta$$

LRFD	ASD
N_u = (105 kips) cos(37.9°) = 82.8 kips	N_a = (70 kips) cos(37.9°) = 55.2 kips

The required flexural load is calculated with Equation 5.

$$M_r = P_r e - N_r\left(\frac{b'}{2}\right)$$

LRFD	ASD
$M_u = (105\,\text{kips})(8\,\text{in.}) - (82.8\,\text{kips})\left(\frac{11.1\,\text{in.}}{2}\right)$ $= 380\,\text{kip-in.}$	$M_a = (70\,\text{kips})(8\,\text{in.}) - (55.2\,\text{kips})\left(\frac{11.1\,\text{in.}}{2}\right)$ $= 254\,\text{kip-in.}$

The combined axial and flexural loads are evaluated with linear interaction according to Equation 3.

$$\frac{N_r}{N_c} + \frac{M_r}{M_c} \le 1.0$$

LRFD	ASD
$I = \frac{N_u}{\phi N_n} + \frac{M_u}{\phi M_n} \le 1.0$ $= \frac{82.8\,\text{kips}}{(0.90)(217\,\text{kips})} + \frac{380\,\text{kip-in.}}{(0.90)(602\,\text{kip-in.})}$ $= 1.13 > 1.0$ **n.g.**	$I = \frac{N_a}{N_n/\Omega} + \frac{M_a}{M_n/\Omega} \le 1.0$ $= \frac{55.2\,\text{kips}}{(217\,\text{kips})/(1.67)} + \frac{254\,\text{kip-in.}}{(602\,\text{kip-in.})/(1.67)}$ $= 1.13 > 1.0$ **n.g.**

The design is unsatisfactory. Using LRFD loads, the elastic normal stress at the critical section, $\sigma = N_u/A + M_u/S$, is 66.4 ksi > 45 ksi.

Finite Element Design Method

IDEA StatiCa software is used with a 5% strain limit. The material resistance and safety factors are assigned to the yield strength.

LRFD	ASD
$\phi = 0.90$	$\Omega = 1.67$

A model conforming with the assumption that the seat plate is connected only to the bracket plate was built.
The Mode 1 buckling factors are

LRFD	ASD
2.76 < 4 **n.g.**	4.14 < 6 **n.g.**

Because the Mode 1 buckling factors are smaller than 4 for LRFD design and 6 for ASD design, bracket plate buckling will occur before yield strength is reached. The buckled shape for Mode 1 is shown in Figure 12.

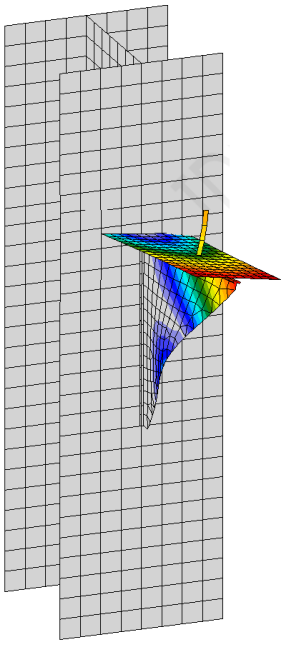

Fig. 12. Mode 1 buckled shape.

The results of materially nonlinear plastic analysis cannot be relied upon. The LRFD maximum equivalent stress in the bracket plate is 45.0 ksi. For this condition, the equivalent stresses are shown in Figure 13.

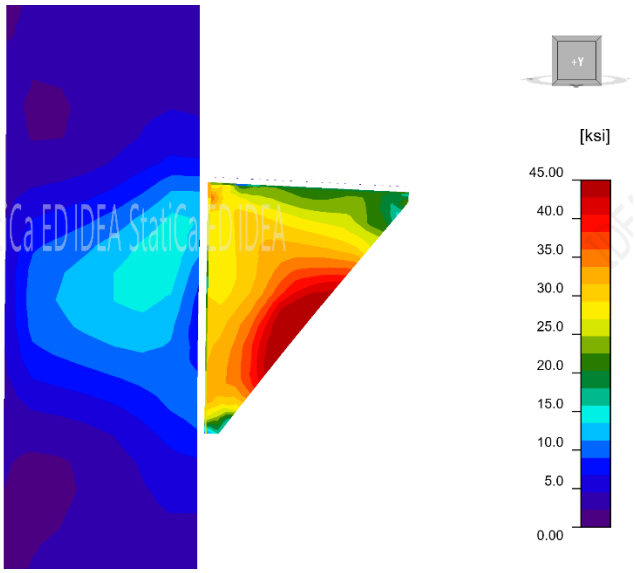

Fig. 13. Equivalent stresses for the model with no seat-plate-to-column weld.

Note that the critical section is not located at the minimum width along the diagonal, perpendicular to the free edge, as is the theoretical assumption, but maximum deflection of the buckling mode shape and maximum stress is located significantly lower on the bracket plate free edge.

Another model was built with the seat plate to column fillet welds. The results are changed significantly.

The Mode 1 buckling factors are

LRFD	ASD
4.34 > 4 **o.k.**	6.51 > 6 **o.k.**

Because the Mode 1 buckling factors are greater than 4 for LRFD design and 6 for ASD design, bracket plate buckling is not an applicable limit state. The buckled shape for Mode 1 is shown in Figure 14.

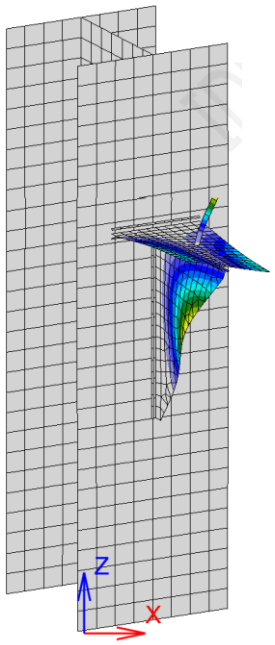

Fig. 14. Mode 1 buckled shape.

The maximum equivalent stresses, σ_{Ed}, in the bracket plate are

LRFD	ASD
33.7 ksi < 45 ksi **o.k.**	22.5 ksi < 30 ksi **o.k.**

Because the maximum equivalent stress is less than the available stress, the bracket plate is in the elastic range and the plastic strain, ε_{Pl}, is 0% < 5 %. The equivalent stresses for LRFD are shown in Figure 15.

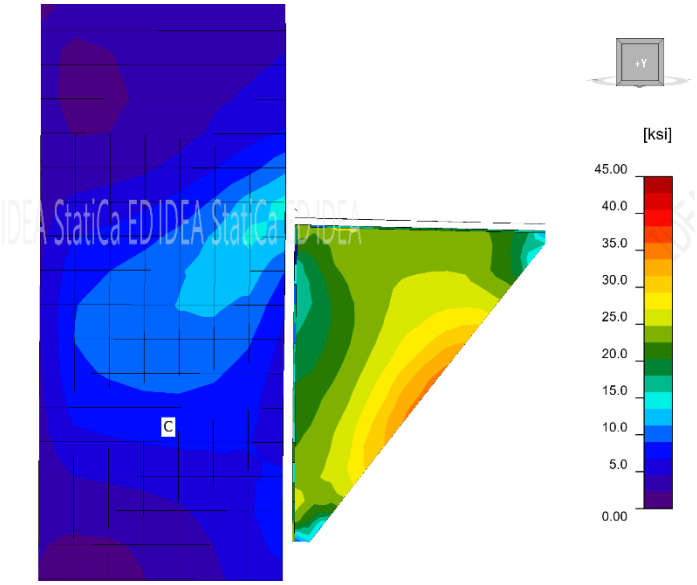

Fig. 15. Equivalent stresses.

The model with the fillet welds between the seat plate to column satisfies the design conditions. The governing limit state is bracket plate buckling, which would occur at the load of 114 kips (LRFD) or 76.0 kips (ASD).

REFERENCES

ABS (2004), *Common Structural Rules for Double Hull Tankers*, Background Document, Section 10-Buckling and Ultimate Strength, Version 14, American Bureau of Shipping, September 14.

AISC (2020), *Task Group Report on Local Buckling (Width-to-Thickness) Limits*, Prepared by the AISC Ad Hoc Task Group on Local Buckling (Width-to-Thickness) Limits, January 7.

AISC (2017), *Steel Construction Manual*, 15th Edition, American Institute of Steel Construction, Chicago, IL.

AISC (2016a), *Specification for Structural Steel Buildings*, ANSI/AISC 360-16, July 7, American Institute of Steel Construction, Chicago, IL.

AISC (2016b), *Prequalified Connections for Special and Intermediate Steel Moment Frames for Seismic Applications*, ANSI/AISC 358-16, May 12, American Institute of Steel Construction, Chicago, IL.

AISC (2011), *Steel Construction Manual*, 14th Edition, American Institute of Steel Construction, Chicago, IL.

AISC (2005), *Steel Construction Manual*, 13th Edition, American Institute of Steel Construction, Chicago, IL.

AISI (2016), *North American Specification for the Design of Cold-Formed Steel Structural Members*, American Iron and Steel Institute, Washington, D.C.

Blodgett, O.W. (1966), *Design of Welded Structures*, The James F. Lincoln Arc Welding Foundation.

Bryan, G.H. (1891), "On the Stability of a Plane Plate Under Thrusts in its Plane, with Applications to the Buckling of the Sides of a Ship," *Proceedings of the London Mathematical Society*, Vol. 22, pp. 54-67.

CEN (2020), Eurocode 3: *Design of Steel Structures-Part 1-14: Design Assisted by Finite Element Analysis*, prEN 1993-1-14, CEN/TC 250/SC 3/WG 22 N 12, Draft Version, May.

CEN (2006), Eurocode 3: *Design of Steel Structures-Part 1-5: Plated Structural Elements*, EN 1993-1-5, October.

CEN (2005), Eurocode 3: *Design of Steel Structures-Part 1-1: General Rules and Rules for Buildings*, EN 1993-1-1, May.

Dowswell, B. (2020), "Gusset Plates: The Evolution of Simplified Design Models," T.R. Higgins Presentation, American Institute of Steel Construction.

Dowswell, B. (2010), "Transfer Forces in Steel Structures," *Engineering Journal*, American Institute of Steel Construction, Third Quarter.

FEMA (2000), *State of the Art Report on Base Metals and Fracture*, FEMA-355A, Federal Emergency Management Agency, September.

Fieber, A., Gardner, L. and Macorini, L. (2019), "Design of Structural Steel Members by Advanved Inelastic Analysis with Strain Limits," *Engineering Structures*, Vol. 199.

Fisher, J.W., Galambos, T.V., Kulak, G.L. and Ravinda, M.K. (1978), "Load and Resistance Factor Design Criteria for Connectors," *Journal of the Structural Division*, American Society of Civil Engineers, Vol. 104, No. ST9, September.

Galambos, T.V. and Ravinda, M.K. (1978), "Properties of Steel for Use in LRFD," *Journal of the Structural Division*, American Society of Civil Engineers, Vol. 104, No. ST9, September, pp. 1459-1468.

Galambos, T.V. and Ravinda, M.K. (1973), *Tentative Load and Resistance Factor Design Criteria for Steel Buildings*, Research Report No. 18, Department of Civil and Environmental Engineering, Washington University, September.

Gerard and Becker (1957), *Handbook of Structural Stability: Volume 1-Buckling of Flat Plates*, National Advisory Committee for Aeronautics, July.

Hall, B.W. and Pekoz, T. (1988), "Probabilistic Evaluation of Test Results," *Ninth International Specialty Conference on Cold-Formed Steel Structures*.

Hess, P.E. Bruchman, D., Assakkaf, I.A. and Ayyub, B.M. (2002), "Uncertainties in Material Strength, Geometric and Load Variables," *Naval Engineers Journal*, Vol. 114, No. 2, April, pp139-166.

Hsu, R.F. (1986), *Analysis of Seat Connection Stiffeners*, MS Thesis, University of Cincinnati, June.

Jensen, C.D. (1936), "Welded Structural Brackets," *Welding Journal*, American Welding Society, October.

Kurikova, M., Wald, F. and Kabelac, J. (2019), "Design of Slender Compressed Plates in Structural Steel Joints by Component Based Finite Element Method," *Proceedings of the Conference on Stability and Ductility of Steel Structures*.

Kurejkova, M. and Wald, F. (2017), "Design of Haunches in Structural Steel Joints," *Journal of Civil Engineering Management*, Vol. 23, No. 6.

Laustsen, B., Nielsen, M.P., Hansen, T. and Gath, J. (2012), "Stability of Brackets and Stiffeners in Steel Structures," *Steel Construction*, Vol. 5, No. 3.

Lee, C.H. (2002), "Seismic Design of Rib-Reinforced Steel Moment Connections based on Equivalent Strut Model," *Journal of Structural Engineering*, American Society of Civil Engineers, Vol. 128, No. 9, September.

Martin, L.H. and Robinson, S. (1981), "Experiments to Investigate Parameters Associated with the Failure of Triangular Steel Gusset Plates," *Joints in Structural Steelwork*, Conference Proceedings, John Wiley & Sons.

Martin, L.H. (1979), "Methods for the Limit State Design of Triangular Steel Gusset Plates," *Building and Environment*, Vol. 14.

Muir and Thornton (2004), "A Direct Method for Obtaining the Plate Buckling Coefficient for Double-Coped Beams," *Engineering Journal*, American Institute of Steel Construction, Third Quarter.

Murray, T.M. and Sumner, E.A. (2003), *Extended End-Plate Moment Connections: Seismic and Wind Applications*, Steel Design Guide 4, Second Edition, American Institute of Steel Construction, Chicago, IL.

Pasternak, H., and Kocker, R. (1995), "Carrying Behavior of Crane Brackets," *Stability of Steel Structures*, Conference Proceedings, Akademiai Kiado.

Robinson, S. (1983), *Failure of Steel Gusset Plates*, Ph.D. Dissertation, Department of Civil Engineering and Construction, The University of Ashton in Birmingham.

Salmon, C.G., and Johnson, J.E. (1990), *Steel Structures: Design and Behavior, Emphasizing Load and Resistance Factor Design*, Third Edition, Harper and Row, New York, New York.

Salmon, C.G., Buettner, D.R., and O'Sheridan, T.C. (1964), "Laboratory Investigation of Unstiffened Triangular Bracket Plates," *Journal of the Structural Division*, American Society of Civil Engineers, Vol. 90, No. ST2, April.

Salmon, C.G. (1962), "Analysis of Triangular Bracket-Type Plates," *Journal of the Engineering Mechanics Division,* American Society of Civil Engineers, Vol. 88, No. EM6, December.

Schmidt, B.J. and Bartlett, F.M. (2002), "Review of Resistance Factor for Steel: Data Collection," *Canadian Journal of Civil Engineering*, Vol. 29, pp. 98-108.

Shakya, S. and Vinnakota, S. (2008), "Design Aid for Triangular Bracket Plates Using AISC Specifications," *Engineering Journal*, American Institute of Steel Construction, Third Quarter.

Seif, M. and Schaefer, B.W. (2010), "Local Buckling of Structural Steel Shapes," *Journal of Constructional Steel Research*, Vol. 66.

Tall, L., Beedle, L.S. and Galambos, T.V. (1964), *Structural Steel Design*, The Ronald Press Company.

Tsai, M. (1992), *Reliability Models of Load Testing*, Ph.D. Dissertation, University of Illinois at Urbana-Champaign.

Winter, G. (1947), "Strength of Thin Steel Compression Flanges," *Transactions of the American Society of Civil Engineers*, Vol. 112, No. 1.

Wu, S.B. and Wang, C.P. (1996), "Analysis of the T-Shaped Stiffened Bracket Plates," *Advances in Steel Structures*, Conference Proceedings, Pergamon.

Ziemian, R.D. (2010), *Guide to Stability Design Criteria for Metal Structures*, Sixth Edition, John Wiley & Sons.

APPENDIX A: EXPERIMENTAL DATA

Table A1. Specimen Details.

Spec.	*b* in.	*a* in.	*t* in.	*e* in.	b_s in.	t_s in.	*E* ksi	σ_y ksi
Salmon et al. (1964)								
1	9.00	12.0	0.386	5.40	15.9	1.72	30,000	43.2
2	22.5	30.0	0.277	13.5	15.9	1.72	30,000	41.2
3	22.5	30.0	0.384	13.5	15.9	1.72	30,000	43.2
4	9.00	9.00	0.268	5.40	15.9	1.72	30,000	41.2
5	9.00	9.00	0.378	5.40	15.9	1.72	30,000	43.2
6	30.0	30.0	0.268	18.0	15.9	1.72	30,000	41.2
7	30.0	30.0	0.385	18.0	15.9	1.72	30,000	43.2
8	13.5	9.00	0.271	8.10	15.9	1.72	30,000	41.2
9	13.5	9.00	0.374	8.10	15.9	1.72	30,000	43.2
10	30.0	20.0	0.276	18.0	15.9	1.72	30,000	41.2
11	30.0	20.0	0.384	18.0	15.9	1.72	30,000	43.2
12	18.0	9.00	0.274	10.8	15.9	1.72	30,000	41.2
13	18.0	9.00	0.387	10.8	15.9	1.72	30,000	43.2
14	30.0	15.0	0.373	18.0	15.9	1.72	30,000	43.2
15	30.0	15.0	0.373	18.0	15.9	1.72	30,000	43.2
Martin (1979)								
1	5.71	5.71	0.240	3.15	5.98	0.240	29,900	43.9
2	5.83	11.6	0.257	4.02	5.94	0.257	29,900	37.4
3	5.94	11.8	0.255	4.06	5.94	0.255	29,900	37.4
4	4.92	4.92	0.254	2.52	4.96	0.254	29,900	37.0
5	4.92	4.92	0.254	2.52	4.96	0.254	29,900	37.0
6	4.80	14.8	0.253	2.56	5.00	0.253	29,900	37.0
7	4.72	14.7	0.254	2.46	5.00	0.254	29,900	37.0
Robinson (1983)								
3-3	7.87	7.87	0.156	3.94	5.91	0.787	29,900	54.8
3-4	7.87	7.87	0.156	3.94	5.91	0.787	29,900	54.8
3-5	11.8	11.8	0.157	5.91	5.91	0.787	29,900	54.8
3-6	15.7	15.7	0.156	7.87	5.91	0.787	29,900	54.8
3-7	15.7	15.7	0.156	7.87	5.91	0.787	29,900	54.8
3-8	19.7	19.7	0.156	9.84	5.91	0.787	29,900	54.8
3-9	19.7	19.7	0.156	9.84	5.91	0.787	29,900	54.8
4-1	7.87	1.97	0.155	3.94	3.94	0.787	29,900	54.8
4-2	7.87	1.97	0.157	3.94	3.94	0.787	29,900	54.8
4-3	7.87	3.94	0.158	3.94	3.94	0.787	29,900	54.8
4-4	7.87	3.94	0.156	3.94	3.94	0.787	29,900	54.8
4-5	7.87	5.91	0.156	3.94	3.94	0.787	29,900	54.8
4-6	7.87	5.91	0.156	3.94	3.94	0.787	29,900	54.8
4-7	7.87	7.87	0.155	3.94	3.94	0.787	29,900	54.8
4-8	7.87	7.87	0.154	3.94	3.94	0.787	29,900	54.8
4-9	7.87	9.84	0.156	3.94	3.94	0.787	29,900	54.8
4-10	7.87	9.84	0.157	3.94	3.94	0.787	29,900	54.8
4-11	7.87	11.8	0.157	3.94	3.94	0.787	29,900	54.8
4-12	7.87	11.8	0.156	3.94	3.94	0.787	29,900	54.8
4-13	7.87	15.7	0.156	3.94	3.94	0.787	29,900	54.8
4-14	7.87	15.7	0.157	3.94	3.94	0.787	29,900	54.8
4-15	7.87	19.7	0.157	3.94	3.94	0.787	29,900	54.8
4-16	7.87	19.7	0.157	3.94	3.94	0.787	29,900	54.8
4-17	7.87	23.6	0.156	3.94	3.94	0.787	29,900	54.8
4-18	7.87	23.6	0.157	3.94	3.94	0.787	29,900	54.8
5-1	11.8	11.8	0.157	2.95	5.91	0.787	29,900	54.8
5-2	11.8	11.8	0.156	3.94	5.91	0.787	29,900	54.8
5-3	11.8	11.8	0.156	5.91	5.91	0.787	29,900	54.8
5-4	11.8	11.8	0.156	5.91	5.91	0.787	29,900	54.8
5-5	11.8	11.8	0.157	7.87	5.91	0.787	29,900	54.8
5-6	11.8	11.8	0.157	9.84	5.91	0.787	29,900	54.8
5-7	11.8	11.8	0.156	11.8	5.91	0.787	29,900	54.8
5-8	11.8	11.8	0.157	11.8	5.91	0.787	29,900	54.8
5-9	11.8	11.8	0.157	11.8	5.91	0.787	29,900	54.8
7-1	11.8	11.8	0.157	5.91	3.94	0.236	29,900	54.8
7-2	11.8	11.8	0.157	5.91	3.94	0.394	29,900	54.8
7-3	11.8	11.8	0.157	5.91	3.94	0.472	29,900	54.8
7-4	11.8	11.8	0.157	5.91	3.94	0.630	29,900	54.8

7-5	11.8	11.8	0.157	5.91	3.94	0.787	29,900	54.8
7-6	11.8	11.8	0.157	11.8	3.94	0.236	29,900	54.8
7-7	11.8	11.8	0.157	11.8	3.94	0.394	29,900	54.8
7-8	11.8	11.8	0.157	11.8	3.94	0.551	29,900	54.8
7-9	11.8	11.8	0.157	11.8	3.94	0.630	29,900	54.8
7-10	11.8	11.8	0.157	11.8	3.94	0.787	29,900	54.8
12-1	11.8	11.8	0.204	5.91	5.91	0.787	29,900	38.1
12-2	11.8	11.8	0.277	5.91	5.91	0.787	29,900	38.1
12-3	11.8	11.8	0.357	5.91	5.91	0.787	29,900	38.1
12-4	11.8	11.8	0.510	5.91	5.91	0.787	29,900	38.1
12-5	11.8	11.8	0.592	5.91	5.91	0.787	29,900	38.1
2-1	11.8	11.8	0.156	5.91	5.91	0.000	29,900	50.8
2-2	11.8	11.8	0.157	5.91	5.91	0.000	29,900	50.8
2-3	11.8	11.8	0.158	5.91	5.91	0.157	29,900	50.8
2-4	11.8	11.8	0.158	5.91	5.91	0.157	29,900	50.8
2-5	11.8	11.8	0.145	5.91	5.91	0.315	29,900	50.8
2-6	11.8	11.8	0.158	5.91	5.91	0.315	29,900	50.8
2-7	11.8	11.8	0.156	5.91	5.91	0.472	29,900	50.8
2-8	11.8	11.8	0.156	5.91	5.91	0.512	29,900	50.8
2-9	11.8	11.8	0.157	5.91	5.91	0.630	29,900	50.8
2-10	11.8	11.8	0.157	5.91	5.91	0.650	29,900	50.8
2-11	11.8	11.8	0.158	5.91	5.91	0.787	29,900	50.8
2-12	11.8	11.8	0.156	5.91	5.91	0.787	29,900	50.8
Kurejkova and Wald (2017)								
A	7.87	15.7	0.236	7.87	10.4	0.787	46.90	23000
B	15.7	15.7	0.236	15.8	10.4	0.787	46.90	23000
C	15.7	15.7	0.157	15.7	10.4	0.787	60.50	23600

E = measured modulus of elasticity, ksi
a = stiffener plate depth, in.
b = stiffener plate width, in.
b_s = seat plate width, in.
e = load eccentricity (see Figure 1), in.
t = stiffener plate thickness, in.
t_s = seat plate thickness, in.
σ_y = measured yield stress, ksi

Table A2. Experimental and Design Results.									
Spec.	P_e kips	b/a	b/t	AISC			FEM		
				Q	P_c kips	P_e/P_c	P_{el}/P_e	P_i kips	P_e/P_i
Salmon et al. (1964)									
1	97.8	0.750	23.3	0.900	49.1	1.99	3.91	61.4	1.59
2	63.3	0.750	81.2	0.137	12.8	4.95	1.02	106	0.597
3	126	0.750	58.6	0.251	34.1	3.69	1.28	151	0.833
4	40.0	1.00	33.6	0.801	20.9	1.91	3.44	29.0	1.38
5	69.5	1.00	23.8	0.949	36.7	1.89	5.06	42.4	1.64
6	49.5	1.00	112	0.095	8.29	5.97	0.85	98.4	0.503
7	102	1.00	77.9	0.187	24.6	4.14	1.19	144	0.706
8	31.3	1.50	49.8	0.695	15.4	2.03	2.92	23.7	1.32
9	64.5	1.50	36.1	0.861	27.6	2.34	3.48	32.0	2.02
10	35.8	1.50	109	0.155	7.77	4.61	1.21	56.2	0.637
11	80.1	1.50	78.1	0.286	20.9	3.83	1.39	82.1	0.976
12	29.8	2.00	65.7	0.598	11.0	2.70	2.29	20.0	1.49
13	46.6	2.00	46.5	0.820	22.4	2.08	3.83	29.3	1.59
14	57.6	2.00	80.4	0.380	16.7	3.45	1.69	48.8	1.18
15	58.5	2.00	80.4	0.380	16.7	3.50	1.66	48.8	1.20
Martin (1979)									
1	28.7	1.00	23.8	0.946	16.7	1.72	6.84	30.0	0.957
2	42.6	0.502	22.7	0.869	19.9	2.15	4.26	30.9	1.38
3	43.7	0.505	23.3	0.857	20.0	2.19	4.25	40.0	1.09
4	30.2	1.00	19.4	1.00	14.9	2.02	9.67	25.4	1.19
5	35.8	1.00	19.4	1.00	14.9	2.40	8.16	25.4	1.41
6	39.6	0.323	19.0	0.893	29.6	1.34	7.85	38.7	1.02
7	47.9	0.322	18.6	0.902	30.8	1.56	6.54	40.8	1.17
Robinson (1983)									
3-3	2.43	2.43	2.43	2.43	8.18	2.43	2.72	37.6	0.529
3-4	2.63	2.63	2.63	2.63	8.12	2.63	2.54	37.6	0.568
3-5	3.20	3.20	3.20	3.20	5.58	3.20	1.98	52.8	0.338
3-6	3.68	3.68	3.68	3.68	4.06	3.68	1.72	62.6	0.238
3-7	3.80	3.80	3.80	3.80	4.09	3.80	1.65	62.6	0.249
3-8	5.54	5.54	5.54	5.54	3.25	5.54	1.10	73.6	0.244
3-9	5.46	5.46	5.46	5.46	3.22	5.46	1.13	73.6	0.239
4-1	2.48	2.48	2.48	2.48	1.95	2.48	11.9	4.13	1.17
4-2	2.53	2.53	2.53	2.53	1.99	2.53	11.9	4.18	1.20
4-3	2.36	2.36	2.36	2.36	5.47	2.36	4.30	10.4	1.24
4-4	2.32	2.32	2.32	2.32	5.34	2.32	4.33	13.2	0.937
4-5	2.63	2.63	2.63	2.63	7.26	2.63	2.80	27.9	0.685
4-6	2.63	2.63	2.63	2.63	7.26	2.63	2.80	27.9	0.685
4-7	2.60	2.60	2.60	2.60	7.99	2.60	2.57	37.7	0.552
4-8	2.50	2.50	2.50	2.50	7.87	2.50	2.67	37.5	0.525
4-9	3.11	3.11	3.11	3.11	8.67	3.11	2.04	45.4	0.594
4-10	2.73	2.73	2.73	2.73	8.86	2.73	2.31	45.7	0.529
4-11	2.75	2.75	2.75	2.75	9.00	2.75	2.28	50.3	0.492
4-12	3.14	3.14	3.14	3.14	8.73	3.14	2.01	50.1	0.547
4-13	2.83	2.83	2.83	2.83	8.86	2.83	2.19	55.9	0.448
4-14	2.77	2.77	2.77	2.77	8.93	2.77	2.27	56.2	0.440
4-15	3.00	3.00	3.00	3.00	8.82	3.00	2.13	59.9	0.441
4-16	3.08	3.08	3.08	3.08	8.75	3.08	2.09	59.9	0.450
4-17	2.78	2.78	2.78	2.78	8.51	2.78	2.32	62.3	0.379
4-18	3.06	3.06	3.06	3.06	8.63	3.06	2.11	62.6	0.422
5-1	1.84	1.84	1.84	1.84	16.5	1.84	3.24	43.0	0.706
5-2	2.54	2.54	2.54	2.54	9.74	2.54	2.60	63.7	0.388
5-3	2.89	2.89	2.89	2.89	5.45	2.89	2.21	52.6	0.299
5-4	2.95	2.95	2.95	2.95	5.45	2.95	2.16	52.6	0.306
5-5	2.96	2.96	2.96	2.96	3.80	2.96	2.03	41.4	0.272
5-6	3.01	3.01	3.01	3.01	2.93	3.01	1.86	32.8	0.269
5-7	2.88	2.88	2.88	2.88	2.34	2.88	1.84	22.9	0.294
5-8	2.63	2.63	2.63	2.63	2.39	2.63	1.97	23.0	0.274
5-9	2.92	2.92	2.92	2.92	2.39	2.92	1.78	23.0	0.303
7-1	3.02	3.02	3.02	3.02	5.54	3.02	1.90	34.1	0.490
7-2	3.05	3.05	3.05	3.05	5.54	3.05	1.95	41.2	0.409
7-3	2.84	2.84	2.84	2.84	5.54	2.84	2.12	43.3	0.363
7-4	4.84	4.84	4.84	4.84	5.58	4.84	1.27	46.4	0.581
7-5	3.17	3.17	3.17	3.17	5.49	3.17	2.03	49.7	0.351
7-6	2.82	2.82	2.82	2.82	2.39	2.82	1.47	5.6	1.21
7-7	2.77	2.77	2.77	2.77	2.39	2.77	1.63	9.3	0.711

7-8	2.84	2.84	2.84	2.84	2.37	2.84	1.68	11.2	0.602
7-9	2.99	2.99	2.99	2.99	2.39	2.99	1.65	15.1	0.473
7-10	2.82	2.82	2.82	2.82	2.39	2.82	1.83	18.7	0.361
12-1	2.21	2.21	2.21	2.21	12.2	2.21	2.33	32.0	0.840
12-2	1.68	1.68	1.68	1.68	28.7	1.68	3.14	42.8	1.13
12-3	2.25	2.25	2.25	2.25	45.0	2.25	3.79	75.1	1.35
12-4	2.30	2.30	2.30	2.30	75.7	2.30	6.03	103	1.69
12-5	2.62	2.62	2.62	2.62	88.9	2.62	6.73	118	1.98
2-1	3.33	3.33	3.33	3.33	5.37	3.33	1.44	17.7	1.01
2-2	4.00	4.00	4.00	4.00	5.58	4.00	1.16	17.8	1.25
2-3	3.77	3.77	3.77	3.77	5.62	3.77	1.47	25.2	0.842
2-4	4.25	4.25	4.25	4.25	5.62	4.25	1.31	25.2	0.948
2-5	4.57	4.57	4.57	4.57	4.38	4.57	1.31	34.8	0.575
2-6	4.17	4.17	4.17	4.17	5.62	4.17	1.42	37.4	0.627
2-7	3.51	3.51	3.51	3.51	5.41	3.51	1.74	41.2	0.461
2-8	3.54	3.54	3.54	3.54	5.37	3.54	1.75	42.0	0.452
2-9	4.08	4.08	4.08	4.08	5.58	4.08	1.51	44.7	0.510
2-10	4.20	4.20	4.20	4.20	5.58	4.20	1.48	45.1	0.520
2-11	3.97	3.97	3.97	3.97	5.62	3.97	1.62	48.1	0.464
2-12	4.47	4.47	4.47	4.47	5.37	4.47	1.44	47.5	0.505
Kurejkova and Wald (2017)									
A	40.6	0.500	33.3	0.404	8.83	4.60	1.34	33.9	1.20
B	24.7	1.00	66.7	0.187	4.65	5.31	0.932	29.9	0.826
C	16.7	1.00	100	0.066	1.42	11.8	0.462	35.1	0.476
The 14 specimens with $P_{el}/P_e \geq 4$ are shaded in green.									